Electronic Supplementary Material (ESI) for Polymer Chemistry.

Supporting Information

Enhanced Thermal and Porous Properties of Double-Decker-Shaped Polyhedral Silsesquioxanes-Bismaleimide (DDSQ-BMI) Nanocomposites for High-Performance CO2 Storage and Supercapacitor

Zih-Yu Chen, Wei-Cheng Chen, and Shiao-Wei Kuo*

Department of Materials and Optoelectronic Science, Center for Functional Polymers and Supramolecular Materials, National Sun Yat-Sen University, Kaohsiung 80424, Taiwan

To whom should be corresponding

E-mail: kuosw@faculty.nsysu.edu.tw

Characterization

FTIR spectra were collected on a Bruker Tensor 27 FTIR spectrophotometer with a resolution of 4 cm^{-1} by using KBr disk method. ^{13}C nuclear magnetic resonance (NMR) spectra was examined by using an INOVA 500 instrument with DMSO as the solvent and TMS as the external standard. Chemical shifts are reported in parts per million (ppm). The curing behavior and thermal stabilities of the samples were performed by using a TG Q-50 thermogravimetric analyzer under a N_2 atmosphere; the cured sample (ca. 5 mg) was put in a Pt cell with heating rate of 20 °C min^{-1} from 100 to 800 °C under a N_2 flow rate of 60 mL min^{-1}. The morphologies of the polymer samples were examined by Field emission scanning electron microscopy (FE-SEM; JEOL JSM7610F) and also by transmission electron microscope (TEM) using JEOL-2100 instrument at an accelerating voltage of 200 kV. BET surface area and porosimetry measurements of samples (ca. 40–100 mg) were measured using BEL Master™/BEL sim™ (v. 3.0.0). N_2 adsorption and desorption isotherms were generated through incremental exposure to ultrahigh-purity N_2 (up to ca. 1 atm) in a liquid N_2 (77 K) bath. Surface parameters were calculated using BET adsorption models in the instrument's software. The pore size of the prepared samples was determined by using nonlocal density functional theory (NLDFT).

Electrochemical Analysis

Working Electrode Cleaning: Prior to using, the glassy carbon electrode (GCE) was polished several times with 0.05-µm alumina powder, washed with EtOH after each polishing step, cleaned through sonication (5 min) in a water bath, washed with EtOH, and then dried in the oven at 50 ^{o}C.

Electrochemical Characterization: The electrochemical experiments were performed in a three-electrode cell using an Autolab potentiostat (PGSTAT204) and 1 M KOH as the aqueous electrolyte. The GCE was used as the working electrode (diameter: 5.61 mm; 0.2475 cm^2); a Pt wire was used as the counter electrode; Hg/HgO (RE-1B, BAS) was the reference electrode. All reported potentials refer to the Hg/HgO potential. A slurry was prepared by dispersing FEC-Mel or FEC-PBDT POPs (2 mg), carbon black (2 mg), and Nafion (10 wt%) in a mixture of (EtOH/ H_2O) (200 µL: 800 µL) and then sonicating for 1 h. A portion of this slurry (10 µL) was pipetted onto the tip of the electrode, which was then dried in air for 30 min prior to use. The electrochemical performance was studied through CV at various sweep rates (5–200 mV s^{-1}) and through the GCD method in the potential range from 0 to -1.00 V (vs. Hg/HgO) at various current densities (0.5–20 A g^{-1}) in 1 M KOH as the aqueous electrolyte solution.

The specific capacitance was calculated from the GCD data using the equation.

$$C_s = (I\Delta t)/(m\Delta V)$$

Where C_s (F g^{-1}) is the specific capacitance of the supercapacitor, I (A) is the discharge current, ΔV (V) is the potential window, Δt (s) is the discharge time, and m (g) is the mass of the NPC on the electrode. The energy density (E, W h kg^{-1}) and power density (P, W kg^{-1}) were calculated using the equations.

$$E = 1000C(\Delta V)^2/(2 \times 3600)$$

$$P = E/(t/3600)$$

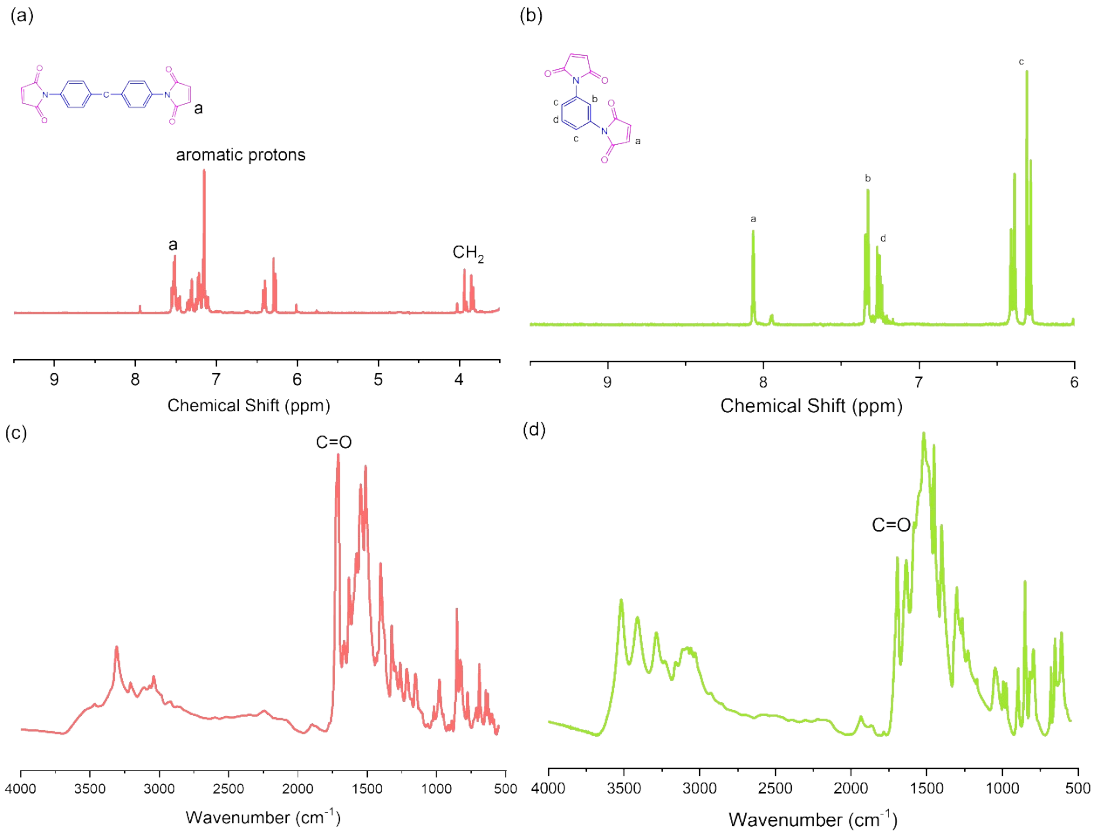

Fig. S1. (a) 1H NMR and (c) FTIR spectra of MDA-BMI and (b) 1H NMR and (d) FTIR spectra of MPD-BMI.

Table S1: EDS results of c-DDSQ-MDA-BMI and c-DDSQ-MPD-BMI

	c-DDSQ-MDA-BMI			c-DDSQ-MPD-BMI		
Element	C	O	Si	C	O	Si
Wt%	35.34	37.13	27.53	35.89	45.07	19.04
Atomic %	35.89	45.07	19.04	15.68	53.99	30.33

Table S2. Comparison the specific capacitance of c-DDSQ-MDA-BMI and c-DDSQ-MPD-BMI with those of previously reported materials for supercapacitor application.

Materials	**SC (F/g)**	**CD**	**CR (%)**	**Ref.**
c-DDSQ-MDA-BMI	73.66	0.5 A/g	86.4	This work
c-DDSQ-MPD-BMI	22.86	0.5 A/g	84.1	This work
Bi_2O_3/Ni foam/graphite/ Asymmetric SC	37	1 mA/cm	-	S1
Bismuth ferrite nanoflake	72.2	1 A/g	82.8	S2
Cz-Cz CMP	43.70	0.5 A/g	98.78	S3
Cz-TP CMP	67.38	0.5 A/g	99.86	S3
pure CNT	15.5	0.5 A/g	-	S4
CoPc/CNT	35	0.5 A/g	-	S4
CS@Bi_2MoO_6	62.55	1 A/g	70	S5
C-S1900	70	2 mV/s	-	S6
Py-BSU CMP	38	0.5 A/g	99.8	S7
TBN-BSU CMP	70	0.5 A/g	99.9	S7
TBN-Py-CMP	31	0.5 A/g	96.98	S8
TBN-TPE-CMP	18.45	0.5 A/g	95.21	S8
TBN-Car-CMP	18.90	0.5 A/g	96.86	S8
TBN-Car-CMP/SWCNT	53	0.5 A/g	96.95	S8

SC: Specific Capacitance, **CD:** Current Density, **CR:** Capacitance Retention.

References

[S1] N.M. Shinde; Q.X. Xia; J.M. Yun; S. Singh; R.S. Mane; K.H. Kim. A binder-free wet chemical synthesis approach to decorate nanoflowers of bismuth oxide on Ni-foam for fabricating laboratory scale potential pencil-type asymmetric supercapacitor device. *Dalton Trans.* **2017**, *46*, 6601–6611, DOI: 10.1039/C7DT00953D

[S2] V.V. Jadhav; M.K. Zate; S. Liu; M. Naushad; R.S. Mane; K.N. Hui; S.H. Han. Mixed-phase bismuth ferrite nanoflake electrodes for supercapacitor application. *Appl. Nanosci.* **2016**, *6*, 511–519, DOI: 10.1007/s13204-015-0469-8

[S3] A.F. Saber; S.U. Sharma; J.T. Lee; A.F.M.; EL-Mahdy; S.W. Kuo. Carbazole-conjugated microporous polymers from Suzuki–Miyaura coupling for supercapacitors. *Polym.* **2022**, *254*, 125070, DOI: 10.1016/j.polymer.2022.125070

[S4] L. Mei; X. Cui; Q. Duan; Y.H. Li; X.L. Lv; H.G. Wang. Metal phthalocyanine-linked conjugated microporous polymer hybridized with carbon nanotubes as a high-performance flexible electrode for supercapacitors. *International Journal of Hydrogen Energy.* **2020**, *3*, 22950–22958, DOI: 10.1016/j.ijhydene.2020.06.208

[S5] K.J. Samdani; J.H. Park; D.W. Joh; K.T. Lee. Self-assembled Bi_2MoO_6 nanopetal array on carbon spheres toward enhanced supercapacitor performance. *ACS Sustainable Chem. Eng.* **2018**, *6*, 16702–16712, DOI: 10.1021/acssuschemeng.8b03988

[S6] P. Su; L. Jiang; J. Zhao; J Yan; C Li; Q Yang. Mesoporous graphitic carbon

nanodisks fabricated via catalytic carbonization of coordination polymers. *Chem. Commun.* **2012**, *48*, 8769–8771, DOI: 10.1039/C2CC34234K

[S7] M.G. Mohamed; S.Y. Chang; M. Ejaz; M.M. Samy; A.O. Mousa; S.W. Kuo. Design and synthesis of bisulfone-linked two-dimensional conjugated microporous polymers for CO_2 adsorption and energy storage. *Molecules* **2023**, *28*, 3234, DOI: 10.3390/molecules28073234

[S8] M.M. Samy; M.G. Mohamed; A.F.M.; EL-Mahdy; T.H. Mansoure; C.W. Wu; S.W. Kuo. High-performance supercapacitor electrodes prepared from dispersions of tetrabenzonaphthalene-based conjugated microporous polymers and carbon nanotubes. *ACS Appl. Mater. Interfaces* **2021**, *13*, 51906–51916, DOI: 10.1021/acsami.1c05720